

## Midinfrared Optical Breakdown in Transparent Dielectrics

D. M. Simanovskii and H. A. Schwettman

*W.W. Hansen Experimental Physics Laboratory, Stanford University, Stanford, California 94305, USA*

H. Lee and A. J. Welch

*Department of Mechanical Engineering and Department of Biomedical Engineering, University of Texas at Austin, Austin, Texas 78712, USA*

(Received 12 March 2003; published 4 September 2003)

Optical breakdown measurements for transparent dielectrics are reported for 1 ps laser pulses as a function of mid-IR wavelength from 4.7 to 7.8  $\mu\text{m}$ . For wide-gap dielectrics seed electrons are generated by tunnel ionization with subsequent avalanche ionization and laser absorption by dense plasma. For narrow-gap dielectrics tunnel ionization alone leads to dense plasma formation.

DOI: 10.1103/PhysRevLett.91.107601

PACS numbers: 77.22.Jp, 79.20.Ds, 42.60.-v, 32.80.Fb

Laser-induced breakdown in transparent dielectric materials has been studied experimentally and theoretically for a wide range of laser pulse durations and wavelengths. During the last decade particular attention has been given to short-pulse laser breakdown in dielectrics with pulses shorter than  $\sim 10$  ps. In this time domain the laser energy is absorbed by electrons faster than it is transferred to the lattice, making the breakdown process dependent mainly on electronic properties of the material. The generally accepted mechanism of dielectric breakdown in this short-pulse regime is the generation of seed electrons by photoionization, either multiphoton ionization (MPI) or tunnel ionization (TI), with subsequent avalanche ionization (AI) and laser energy absorption by dense plasma. The relative role of these ionization processes depends on material properties and on the laser pulse duration and wavelength. At near-infrared wavelengths, and pulse lengths between 100 fs and 10 ps, MPI generates a sufficient number of free electrons to initiate the avalanche process [1–3]. For pulses shorter than 100 fs, TI becomes important and the total number of electrons produced by photoionization increases [4,5]. There are indications that for pulses approaching 5 fs, plasma of critical density can be generated solely by TI [6,7].

The short-pulse laser-induced breakdown studies, referred to above, were performed in a relatively narrow spectral range at wavelengths shorter than 1053 nm. The present work extends these breakdown studies into the mid-IR spectral region to wavelengths as long as 8000 nm. At mid-IR wavelengths MPI is strongly suppressed since many tens of photons are required to excite electrons across the band gap of typical dielectrics. One can expect, therefore, significant differences in the breakdown process. For a fixed pulse length of 1 ps, we have measured the mid-IR spectral dependence of the optical breakdown threshold for a number of dielectric materials with different band gaps.

For the optical breakdown experiments we used two laser sources: a commercial Ti:sapphire (Ti:S) laser for

measurements at 400 and 800 nm (we will call these “visible light” experiments), and an optical parametric amplifier (OPA) for mid-IR measurements. Pulses of mid-IR radiation, tunable from 4 to 8  $\mu\text{m}$  with energy up to 1  $\mu\text{J}$  and pulse length of 1 ps, were generated in a commercial OPA pumped by a Ti:S laser system (OPA-800, Spectra Physics). These pulses were further amplified in an AgGaS<sub>2</sub>-based OPA, pumped by a Nd:YLF laser at 1053 nm. AgGaS<sub>2</sub> is one of the most efficient nonlinear materials transparent in the mid-IR, but it cannot be pumped directly by a Ti:S laser near 800 nm because of two-photon absorption [8]. It can be efficiently pumped, however, by a Nd: laser at 1053 nm, since its band edge is close to 450 nm and two-photon absorption vanishes. To generate such pump pulses we used a Nd:YLF linear amplifier seeded by frequency shifted Ti:S laser pulses. A fraction of the Ti:S laser pulse used for OPA pumping (300  $\mu\text{J}$ ) was frequency shifted in a methane filled Raman converter from 805 to 1053 nm in order to match the amplification band of the Nd:YLF crystal. Converted pulses with energy of about 30  $\mu\text{J}$  were amplified in a double-pass flash lamp pumped Nd:YLF amplifier to the level of 1.5 mJ. These pulses were used as pump pulses for the AgGaS<sub>2</sub> mid-IR amplifier, which generated picosecond mid-IR pulses with energies up to 50  $\mu\text{J}$  tunable from 4.7 to 7.8  $\mu\text{m}$ . The system was operated at 10 Hz.

The delivery and detection optics employed in our breakdown studies is illustrated schematically in Fig. 1. The configuration is similar to that used in previous breakdown studies [9]. To reach the high fluences required for dielectric breakdown in transparent materials, laser pulses were focused with a two mirror system with NA = 0.25. The focal spot size, which was close to diffraction limited, varied with wavelength and was measured by a knife-edge method for all wavelengths used in our study. It ranged from  $12 \pm 1.5 \mu\text{m}$  at 4.7  $\mu\text{m}$  wavelength to  $18 \pm 2 \mu\text{m}$  at 7.8  $\mu\text{m}$ . The maximum achievable fluence at the top of the intensity distribution in the focal spot exceeded 20 J/cm<sup>2</sup>, well above damage threshold for all

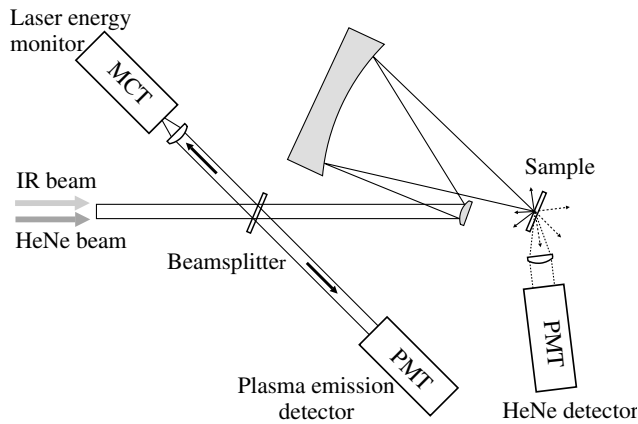


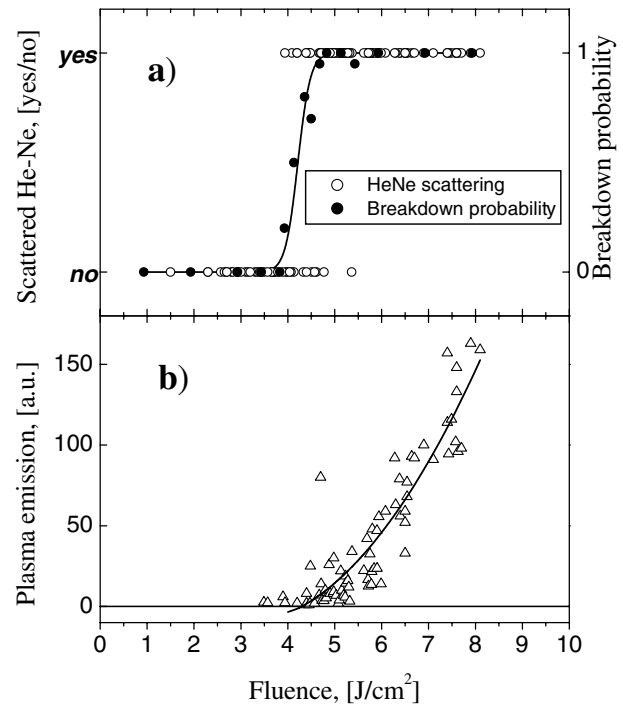
FIG. 1. Schematic of optical apparatus.

tested materials. The energy of each pulse was monitored with a room temperature mercury cadmium telluride (MCT) detector calibrated for each wavelength using a laser power meter (Ophir Optonics). Accuracy of the fluence measurements was determined mainly by the accuracy of the focal spot size measurements and was  $\pm 20\%$ .

The single pulse damage threshold was determined as any surface modification detectable under a visible light microscope. As shown in Fig. 1, two diagnostics were used for *in situ* monitoring of surface damage: scattering of a He-Ne laser beam from the damaged region of the sample, and visible light plasma emission. We found that even the smallest damage observable with the microscope produces significant scattering of the He-Ne beam focused on the optical quality sample surface. Visible light plasma emission also proved to be a good indicator of the damage threshold. Plasma emission from the focal spot region was collected by the same mirror system used to focus the mid-IR light and detected by a photomultiplier tube. The typical dependence of He-Ne scattering and visible light plasma emission on mid-IR fluence is shown in Fig. 2. Each data point in these plots was taken on a new spot on the sample. The breakdown probability distribution calculated from the HeNe scattering data, shown in Fig. 2(a), indicates a mean breakdown fluence of  $4.25 \text{ J/cm}^2$  and a 10% to 90% width of  $\pm 6\%$ . The observed threshold for visible light plasma emission, as shown in Fig. 2(b), occurs at the same fluence within a similar uncertainty.

Both wide-gap and narrow-gap transparent dielectric materials were investigated in the mid-IR optical breakdown experiments. Materials employed in the study are listed in Table I together with their known band gaps. All material samples were optically polished.

Single pulse breakdown threshold measurements for both wide-gap and narrow-gap dielectric materials and for both the visible light and mid-IR spectral regions are presented in Fig. 3. Our data for visible light breakdown of wide-gap dielectrics correspond well to data in the literature where it is found that the threshold increases

FIG. 2. Scattered He-Ne light and plasma emission from a  $\text{CaF}_2$  target irradiated by 1 ps laser pulses at  $6.25 \mu\text{m}$ .

with wavelength since more and more photons are required for MPI. While absolute values of our measured single pulse thresholds are approximately 2 times higher than the multiple pulse thresholds previously reported [2], this factor of 2 ratio of single pulse to multiple pulse thresholds is well known [4,5]. Behavior in the mid-IR is quite different. For wide-gap materials, as seen in Fig. 3, the threshold decreases with increasing wavelength. It is obvious that MPI will be dramatically suppressed for wide-gap materials in the mid-IR. Even at  $4.7 \mu\text{m}$  more than 30 photons are required to produce a free electron. Despite this, there is good evidence that photoionization, through the mechanism of tunnel ionization, plays an important role in the mid-IR breakdown of these materials. As we have already shown in Fig. 2, the mid-IR breakdown threshold width is quite narrow, approximately  $\pm 6\%$ . In the literature a well-defined breakdown threshold has generally been explained by assuming that MPI of bulk material produces a sufficient number of initial electrons to trigger AI. Since we observe similar

TABLE I. Dielectric materials used in experiments.

Group	Material	Band gap $\Delta E$ , eV
Wide-gap materials	LiF	13.6
	MgF <sub>2</sub>	10.8
	CaF <sub>2</sub>	10.0
	BaF <sub>2</sub>	9.07
Narrow-gap materials	ZnS	3.5
	ZnSe	2.7

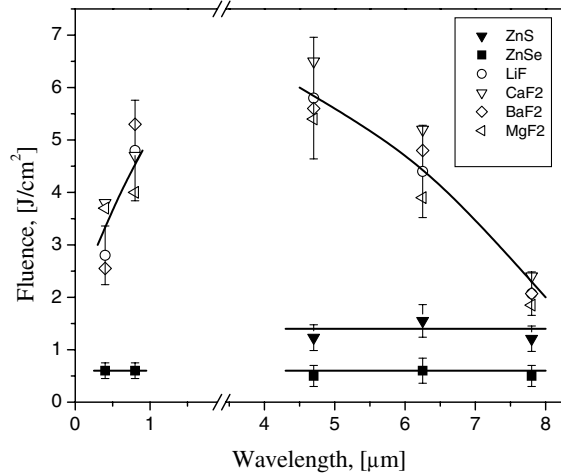


FIG. 3. Wavelength dependence of the breakdown threshold for wide- and narrow-gap materials. Solid lines show general trend of the breakdown thresholds.

threshold widths throughout the visible light and mid-IR regions, it is plausible that TI provides an adequate source of initial electrons in the mid-IR region, just as MPI provides that source in the visible light region.

To assess the likely role of TI in the mid-IR breakdown process, let us evaluate the parameter  $\gamma$  from the Keldysh theory of photoionization [10], which indicates whether ionization proceeds in the multiphoton or the tunneling regime. Photoionization in a strong laser field occurs in the tunneling regime when the parameter  $\gamma \ll 1$ . For solid materials  $\gamma = \frac{\omega \cdot (m \cdot \Delta E)^{1/2}}{e \cdot E}$ , where  $\omega$  is the laser frequency,  $\Delta E$  is the band gap,  $m$  is the electron-hole reduced mass, and  $E$  is the laser electric field. Using the free electron mass, we can give an upper estimation of the parameter  $\gamma$  at damage threshold. For the wide-gap materials studied, the parameter  $\gamma$  is  $\sim 0.4$  for all mid-IR wavelengths. Spectroscopic measurements indicate [7] that TI can prevail in solids at values of  $\gamma$  even larger than 1, solidifying our conclusion about the major role of TI in the breakdown process.

Tunnel ionization is independent of wavelength and thus cannot itself explain the observed decrease in the breakdown threshold with increasing wavelength. This behavior, however, can be attributed to the AI process, once free electrons generated by TI initiate it. For AI the breakdown strength of dielectric materials decreases for low frequencies, with a threshold field approaching its dc value as  $E^{ac}(\omega) = E^{dc}(1 + \omega^2 \tau^2)^{1/2}$ , where  $E^{ac}(\omega)$  is the ac breakdown field,  $E^{dc}$  is the dc breakdown field,  $\omega$  is the laser frequency, and  $\tau$  is the electron collision time [11]. Neither the dc breakdown field, nor the electron collision time are known for the materials studied here; however, taking plausible values ( $E^{dc} \sim 10$  MV/cm and  $\tau \sim 10$  fs) [12] leads to a breakdown fluence of  $\sim 3$  J/cm<sup>2</sup> at a wavelength of  $6 \mu\text{m}$ . This estimated breakdown fluence, which is proportional to  $(E^{ac})^2$ , is within 50% of the measured value.

Evidence of the TI-initiated avalanche breakdown of wide-gap materials also can be found in the morphology of the damage spot. In Fig. 4(a) a scanning electron microscope image of the damage spot on MgF<sub>2</sub> is shown. The damage was produced at laser intensity 1.5 times the threshold value. The damage spot consists of a large number of small pits elongated in the direction of the laser electrical field vector. These pits, associated with “weak” points on the surface, such as digs and scratches, served as starting points for the breakdown process. This is quite natural, since the laser electric field is enhanced at such defects and material band structure can also be altered in these regions providing favorable conditions for producing seed electrons by TI that initiate the electron avalanche. Particularly interesting is the elongated shape of these pits. Typical values of eccentricity are somewhat less than  $1 \mu\text{m}$ . In an electric field of several tens of MeV/cm, which corresponds to the threshold intensities, the drift velocity of free electrons is determined by collisions and is almost saturated with a typical value  $v \sim 2 \times 10^7$  cm/s. This velocity multiplied by the laser pulse duration of 1 ps gives us a drift distance that is a fraction of  $1 \mu\text{m}$ , which corresponds quite well to the eccentricity of the observed pits. This observation provides direct evidence of the electron avalanche, which is an essential part of the breakdown process in wide-gap materials.

For narrow-gap materials the mid-IR breakdown threshold is reduced and is independent of wavelength within experimental uncertainty. The observed wavelength independent thresholds for narrow-gap materials might be understandable if TI alone were sufficient to induce breakdown. In the absence of a theory for solid materials we have estimated the rate of tunnel ionization using a parameter called the appearance intensity,  $I_{app}$ , which was introduced [11] to describe the ionization of atoms in a strong laser field. Calculated in the barrier-suppression model, the appearance intensity is  $I_{app} = 4 \times 10^9 E_i^4 / Z^2$  W/cm<sup>2</sup>, where  $Z$  is the ion charge and  $E_i$  is the ionization potential. Using the band gap value in place of the ionization potential and setting the ion charge to 1 for

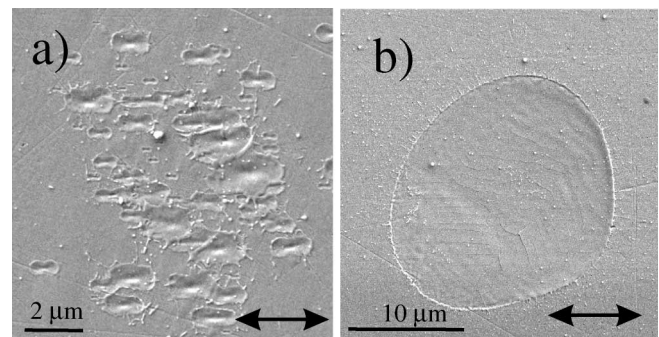


FIG. 4. Scanning electron microscope images of the damage spots on MgF<sub>2</sub> (a) and ZnS (b). Laser wavelength is  $6.25 \mu\text{m}$ . Arrows show direction of the laser electric field.

single stage ionization, we calculated values of the appearance intensity for narrow-gap materials that are 2 to 3 times lower than the observed breakdown threshold intensities. Thus it seems plausible that tunnel ionization could be solely responsible for mid-IR laser breakdown of narrow-gap materials. It should be noted that the ratio of breakdown fluences for the narrow-gap materials ZnSe and ZnS, as shown in Fig. 3, is 2.65. This is also the ratio of breakdown intensities. In plausible agreement with the appearance intensities argument the ratio of band gaps raised to the fourth power is  $(3.5/2.7)^4 = 2.82$ .

The proposition that the optical breakdown process in wide-gap materials is seeded by TI but driven by AI, while the process in narrow-gap materials is driven entirely by TI, is quite reasonable. The appearance intensity depends on the band gap value as  $\Delta E^4$ . On the other hand, the intensity necessary to keep the avalanche coefficient constant scales as  $\Delta E^2$ . This follows from Thornber's model for impact ionization [13], which predicts that in the high intensity limit the avalanche coefficient is proportional to  $I^{1/2}/\Delta E$ . These different scaling laws lead one to the conclusion that for materials with band gap values below some critical value TI becomes more efficient than AI. This conclusion is also supported by morphology data for narrow-gap materials. In Fig. 4(b) a typical scanning electron microscope image of the damage spot on ZnS is shown. The damage spot on narrow-gap materials is smooth and homogeneous, showing no signs of the avalanche related pits found on all wide-gap materials.

In summary, we measured the picosecond single-shot damage thresholds of transparent dielectrics for mid-IR radiation from 4.7 to 7.8  $\mu\text{m}$ . We found that for narrow-

gap materials with  $\Delta E \sim 3$  eV tunnel ionization leading to dense plasma formation is solely responsible for dielectric breakdown. For wide-gap materials with  $\Delta E \sim 10$  eV tunnel ionization provides seed electrons, but optical breakdown is dominated by avalanche ionization.

This work was funded in part by the Air Force Office of Scientific Research under Grant No. F49620-00-1-0349.

- 
- [1] D. Du, X. Liu, G. Korn, J. Squir, and G. Mourou, *Appl. Phys. Lett.* **64**, 3071 (1994).
  - [2] B. C. Stuart, M. D. Feit, S. Herman, A. M. Rubenchik, B. W. Shore, and M. D. Perry, *Phys. Rev. B* **53**, 1749 (1996).
  - [3] P. P. Pronko, P. A. VanRompay, C. Horvath, T. Juhasz, X. Liu, and G. Mourou, *Phys. Rev. B* **58**, 2387 (1998).
  - [4] M. Lenzner, J. Kruger, S. Sartania, Z. Cheng, Ch. Spielman, G. Mourou, W. Kautek, and F. Krausz, *Phys. Rev. Lett.* **80**, 4076 (1998).
  - [5] A. C. Tien, S. Bakus, H. Kapteyn, M. Murnane, and G. Mourou, *Phys. Rev. Lett.* **82**, 3883 (1999).
  - [6] F. Quere, S. Guizard, and Ph. Martin, *Europhys. Lett.* **56**, 138 (2001).
  - [7] M. Peterson, R. Zadoyan, J. Eloranta, N. Schwenter, and V. A. Apkaryan, *J. Phys. Chem. A* **106**, 8308 (2002).
  - [8] P. Hamm and C. Lauterwasse, *Opt. Lett.* **18**, 1943 (1993).
  - [9] Ming Li, Sipriya Menon, John P. Nibarger, and George N. Gibson, *Phys. Rev. Lett.* **82**, 2394 (1999).
  - [10] L. V. Keldysh, *Sov. Phys. JETP* **20**, 1307 (1965).
  - [11] S. Augst, D. Strickland, D. D. Meyerhofer, S. L. Chin, and J. H. Eberly, *Phys. Rev. Lett.* **63**, 2212 (1989).
  - [12] D. Arnold, E. Cartier, and D. J. DiMaria, *Phys. Rev. B* **49**, 10278 (1994).
  - [13] K. K. Thornber, *J. Appl. Phys.* **52**, 279 (1981).